Reactions of complex metalloproteins studied by protein-film voltammetry

Fraser A. Armstrong, Hendrik A. Heering and Judy Hirst

Inorganic Chemistry Laboratory, Oxford University, Oxford, UK OX1 3QR

CHEMICAL SOCIETY REVIEWS

The following review explores applications of voltammetric methods for observing reactions of complex metalloproteins. Attention is focused upon the technique of 'protein-film voltammetry', in which the protein molecules under investigation are adsorbed on the electrode surface and electrochemically 'interrogated.' The experiments address a minuscule sample with high sensitivity, and optimal control over both potential and time dependence of reactions. Factors governing the voltammetric response are outlined, and particular emphasis is given to the ability to study reactions that are coupled to and may 'gate' the primary electron exchange processes. Examples described include proton-transfer and metal-binding reactions of iron–sulfur clusters, coupling of electron transfer in peroxidases, quantifying electron-transport pathways in multi-centred enzymes, and detection of 'switches' that modulate the catalysis as a function of potential.

1 Introduction

Dynamic electrochemical methods are an obvious yet largely unexplored approach to studying redox-active sites in proteins. Consequently, we write this Review with the aim of identifying opportunities afforded by techniques such as cyclic voltammetry for elucidating the complex reactions of biological redox systems. The approach we will describe stems from the original discoveries of Hill and of Kuwana and their coworkers[1,2] who first demonstrated reversible, diffusion-controlled voltammetry of cytochrome c at a solid electrode without mediators and with no sign of denaturation. The all-important feature is application of a controlled electrochemical potential which is varied either continuously or in steps or pulses: this activates specific redox centres, the reactions of which are measured simultaneously through the current response, thereby procuring interdependent thermodynamic and kinetic information from a single set of experiments. The interactive nature of the experiments is optimised by confining the sample under investigation to the electrode surface, in a configuration which we refer to as 'protein-film voltammetry' and upon which we will focus our discussion. In this way, limitations due to the complex and sluggish diffusion of irregular macromolecules to an electrode surface are avoided. The cartoon in Fig. 1 depicts the 'ideal' case—a homogeneous electroactive monolayer of protein molecules—which, at a coverage of between 10^{-11} and 10^{-12} mol cm^{-2}, enables minuscule quantities of sample, often in scarce supply, to be studied. As will be evident, the sharpness and finite nature of the voltammetric response observed for surface-confined redox couples compensates for the resulting low Faradaic currents. The information obtained is wide ranging, beginning most fundamentally with interfacial electron-transfer kinetics, coupled chemical equilibria in labile

Fraser Armstrong gained his PhD in 1978 at the University of Leeds under the supervision of Professor A. G. Sykes. He then held a Royal Society European Exchange Fellowship with Professor Peter Kroneck at Universität Konstanz, Germany. After postdoctoral research with Professors R. G. Wilkins (New Mexico State University), Helmut Beinert (Wisconsin) and Allen Hill (Oxford) he took up a Royal Society University Research Fellowship at Oxford in 1983. In 1989 he joined the faculty at the Department of Chemistry, University of California, Irvine. He returned to Oxford in 1993, where he is currently University Lecturer and a Fellow of St. John's College. His interests are in bioinorganic redox chemistry, in particular the application of physical methods to detect and measure unusual reactivities and to characterise transient or unstable species.

Hendrik (Dirk) Heering received his undergraduate education in Molecular Sciences at the Agricultural University, Wageningen, The Netherlands in 1990. He obtained his PhD in 1995 for studies in bio-electrochemistry under the supervision of Professors W. R. Hagen and C. Veeger at Wageningen. He is currently carrying out postdoctoral research with Fraser Armstrong at Oxford University.

Judy Hirst is from Yorkshire and graduated in chemistry from St. John's College, Oxford in 1994 after working with Professor Richard Compton for a year on photoelectrochemistry. She is currently Senior Scholar at Lincoln College and is completing a doctorate under the supervision of Fraser Armstrong.

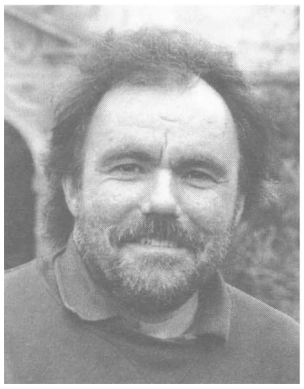

Fraser A. Armstrong

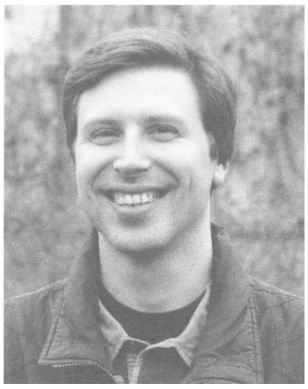

Hendrik A. Heering

Judy Hirst

centres, and kinetics of gated electron-transfer reactions, and, at the most complex level, the organisation of catalytic electron transfer in multicentred redox enzymes. It is easy to forget that one is also able simply to measure reduction potentials!

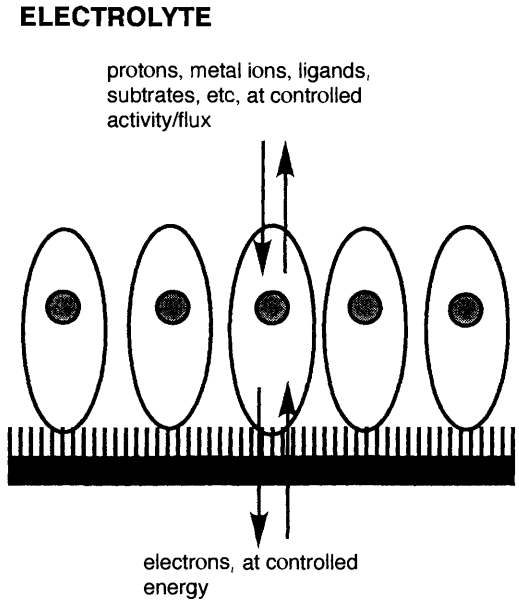

Fig. 1 An idealised configuration for protein-film voltammetry. The protein molecules are arranged as a perfect monolayer, each behaving independently. They interact non-covalently with functionalities on the electrode surface to produce orientations allowing facile interfacial electron exchange and interaction with agents in the contacting electrolyte.

2 Interpreting voltammograms

2.1 Reversible and coupled electron transfer

The majority of studies on adsorbed proteins have been carried out using cyclic (linear sweep) voltammetry which is the most 'visual' of dynamic methods, revealing potential (E) and time perspectives in the simplest way. The scope for studying redox-active sites and their reactions by analysing the voltammetric waveform is illustrated in Fig. 2. Three situations are considered, each of which is simplified by being reversible in terms of interfacial electron transfer: they differ in how this is coupled to further chemical processes.

Fig. 2(a) shows the voltammogram expected for a simple, uncoupled, reversible electron transfer for a surface-confined species. We use the term 'reversible' in the electrochemical sense to indicate that reduced and oxidised forms remain in Nernstian equilibrium throughout the cycle. The reductive and oxidative waves are symmetrical, and currents reach a maximum value at the formal reduction potential $E°'$, thereafter decreasing to zero as the finite number of redox centres are transformed. The separation between peaks (ΔE_p) is zero, the half-height peak width δ is 3.53 RT/nF (83 mV at 0 °C) and the peak current $i_p = n^2F^2\nu A\Gamma/RT$ (ν is the scan rate, n is the number of electrons being transferred, A is the electrode area and Γ is the surface coverage).[3] Obviously, a co-operative two-electron reaction gives rise to a much more prominent signal since i_p is proportional to n^2 and δ varies as $1/n$. Integration gives the number of electrons transferred and hence direct calculation of the electrode coverage (peak area = $nFA\Gamma$). For a protein of molecular mass 100 000, maximum (monolayer) coverage is in the region of 3×10^{-12} mol cm^{-2}.

An example of what happens when the electron transfer is coupled to a non-catalytic chemical reaction is shown in Fig. 2(b). This extension is described generally in terms of the square-scheme model[4,5] where the electrochemical and chem-

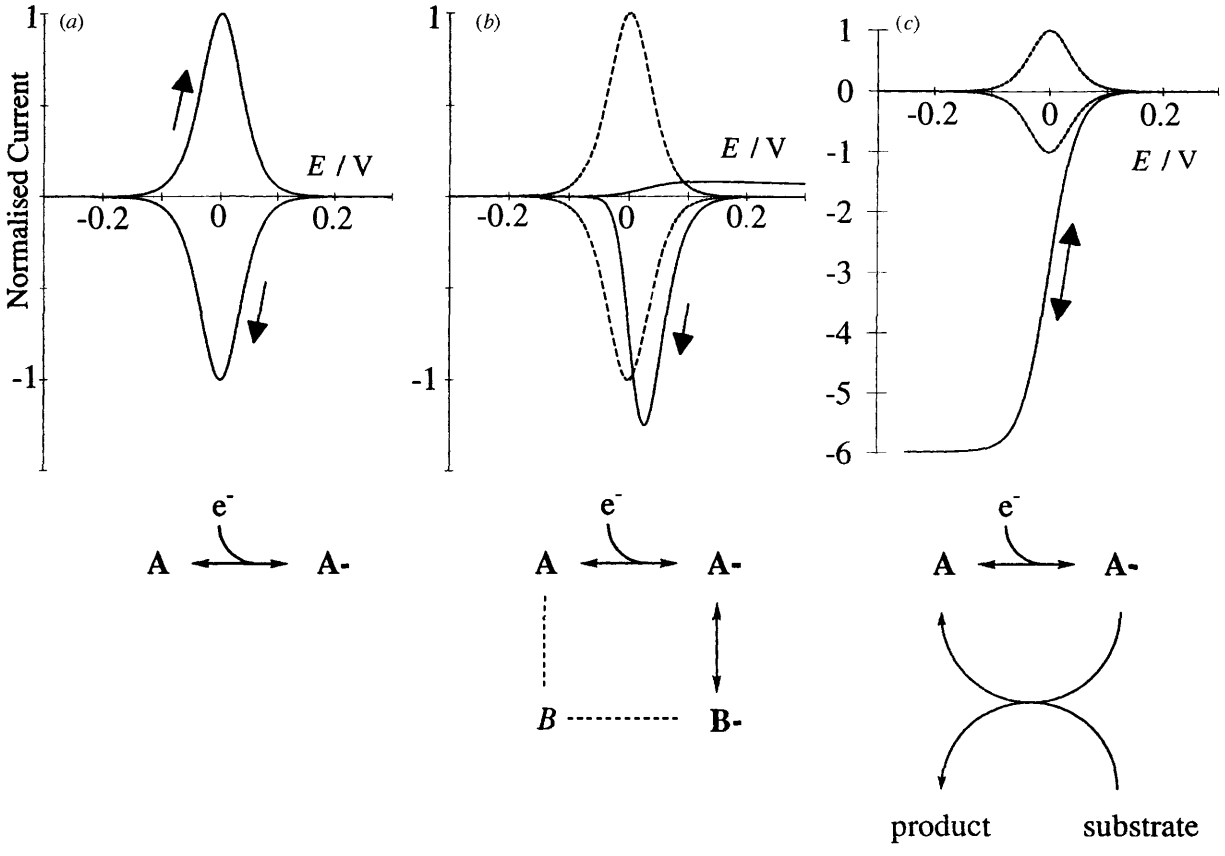

Fig. 2 (a) The ideal response expected from a monolayer of adsorbed electroactive species when the electron transfer is reversible. Currents are presented normalised to $n^2F^2\nu A\Gamma/RT$. (b) A possible response obtained when the electron transfer is followed by chemical conversion to a more stable electroinactive species. (c) Conversion of a one-electron reversible wave to a one-electron reversible catalytic wave on addition of substrate.

ical reactions are assumed to occur separately and are represented respectively by horizontal and vertical co-ordinates. A redox reaction is said to be 'gated' when its rate is controlled by a chemical reaction (vertical transition) rather than by the mechanics of elementary electron transfer (horizontal transition). The kinetics of these chemical transformations are investigated by varying the experimental timescale, for example by changing the concentration of a species involved in a bimolecular step, or, more importantly, by using different potential scan rates. Voltammetry is therefore the obvious and direct method for detecting and deconvoluting gated redox reactions. The situation depicted is one in which the time constant for interconversion between reduced state A^- and the more stable successor species B^- is comparable with the experimental timescale, and B^- is electroinactive within the experimental potential range. Obviously, the reductive and oxidative scans are no longer symmetrical and the reduction potential now reflects the thermodynamic characteristics of the diagonal interconversion between A and B^- instead of the elementary electron exchange $A \leftrightarrow A^-$. The reductive wave is shifted to higher potential and sharpened as the Nernstian equilibrium is 'pulled over' by removal of A^-; conversely the re-oxidation of B^- is gated because it must first convert to A^-. Species A^- is metastable, and although such states may have functional relevance, we note that they might escape detection by conventional (slow) potentiometric methods.[6] An example is described later (Fig. 9 and 10). As the scan rate is lowered, the waves eventually become symmetrical and the reduction potential reflects a thermodynamic distribution of species.

Fig. 2(*c*) shows the voltammetry expected when reversible electron transfer is coupled to catalytic turnover. The active site is electrochemically transformed (in this case it is reduced) and then restored (re-oxidised) to the initial state by substrate, the mass transport of which can be controlled hydrodynamically, most obviously by rotating the electrode. Electrons are thus no longer confined to the adsorbed protein film, and the balance produced between electrochemical and catalytic redox transformation of the active sites results in a steady-state current-potential response. (Note that rotating the electrode does not affect signals from the adsorbed centres in the absence of catalytic turnover). The current relates to the rate of electron transport through the enzyme, and the standard kinetic parameters (k_{cat}, K_M) can be determined from the dependence of limiting currents on rotation rate and substrate concentration.[7] For more complex systems, such as those containing several redox sites, the shape and position of the steady-state catalytic wave reveal subtleties of intramolecular electron transport. One item of interest is how the effective '*n*-value' (the gradient of a plot of $\log\{(i_{lim} - i)/i\}$ *vs.* E) varies with potential and reflects the patterns of redox equilibration along the electron-transfer chain comprising [substrate–enzyme centres–electrode]. The complete catalytic *i–E* dependence will be referred to throughout as the catalytic waveform and may comprise multiple waves having different waveshapes.

Cyclic voltammetry provides a 'wide-angle' picture of complex redox chemistry; for example each of the cases A, B and C can be selectively accessed by correct choice of conditions (such as supply and concentration of substrate, and experimental timescale). However, there are drawbacks: for example, the sensitivity of analogue linear-sweep voltammetry is low [*i.e.* signals for non-catalytic (*i.e.* un-amplified) reactions are small], and use of a potential modulation, for example as in square-wave voltammetry, can significantly raise detection limits.[8] Other methods offer advantages for deconvoluting the potential and time domains. Thus, whereas extraction of transient kinetic data from a cyclic voltammogram requires simulation procedures, potential-step methods, *i.e.* chronoamperometry and chronopotentiometry, remove the potential domain and yield direct measurement of rates. These techniques are viable for adsorbed proteins, just as they have been used for small molecule systems (see below).[9,10] Methods based on impedance, using frequency to impose the time domain, have also been used to measure electron-transfer rates of adsorbed species, with the advantage that large potential excursions are not involved.[11,12]

3 'Simple' voltammetry: theory and experiment

3.1 Marcus theory and electrochemical rates

The 'reversible' electrochemistry assumed above is obviously an idealistic notion, and voltammetric waveforms must under certain conditions (*e.g.* sluggish electron transfer, high scan rates) become sensitive to the kinetics of interfacial electron exchange. Use of protein-film voltammetry to investigate complex redox reactions of proteins necessitates that the interfacial electron-exchange characteristics be defined. Major recent developments in the understanding of interfacial electron transfer between an electrode and adsorbed species stem from studies of systems having acceptable structural definition, and in particular from the application of Marcus theory.[13] The more traditionally used Butler–Volmer formulism[3] takes no account of the nature of the electronic states involved, and two major assumptions are made. First, it is assumed that the reaction surface is linear, so that potential energy varies linearly rather than parabolically along the reaction co-ordinate, and secondly, all electrode energy levels apart from the Fermi level are ignored. As a result, the variation of electrochemical rate constants with overpotential is incorrect: Butler–Volmer theory predicts an ever (exponentially) increasing electrochemical rate constant, whereas in fact (and correctly predicted by Marcus theory) the rate reaches a constant level (independent of applied potential) at high overpotential, as shown in Fig. 3. This 'plateau' is the electrochemical equivalent of the inverted region.[9] Rate constants at large overpotential are thus greatly over-estimated by the Butler–Volmer model.

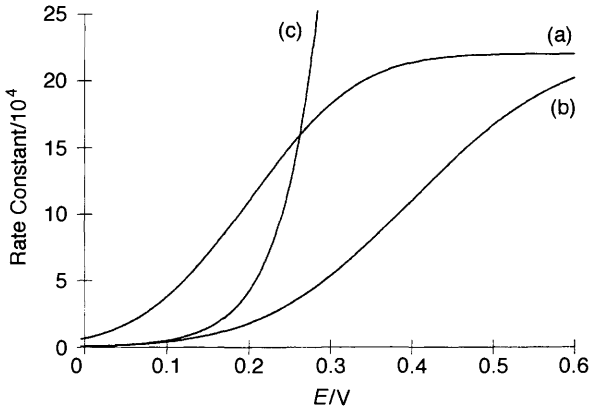

Fig. 3 Comparison of electrochemical rate constants predicted by Marcus and Butler–Volmer theories. (a) and (b): Marcus theory rate constants for small (0.2 eV) and larger (0.4 eV) reorganisation energies respectively, the same plateau level (2×10^5 s^{-1}) is achieved in each case. (c): the Butler–Volmer dependence with k_0 the same as for (b).

Butler–Volmer theory thus predicts that even a very sluggish electron-transfer reaction should exhibit a sharp waveform (since the electron-transfer rate increases exponentially), the irreversible limiting value for δ being $62.5/\alpha$ mV at 25 °C, *i.e.* 125 mV for α (transfer coefficient) = 0.5. Broadening arises from non-ideality, an obvious example being kinetic dispersion in which different orientations of molecules display a spectrum of rate constants.[12] However, Marcus theory predicts broadening even for an ideal, homogeneous array since the rate of a process having a small reorganisation energy quickly ceases to respond to an increase in driving force. This is illustrated in Fig. 4, which compares waveshapes expected, in such a situation, for Butler–Volmer and Marcus models having the same value of k_0. For cyclic voltammetry, the interfacial electron-transfer kinetics can be measured by analysing how peak positions vary with scan rate.[14,15] The Marcus model

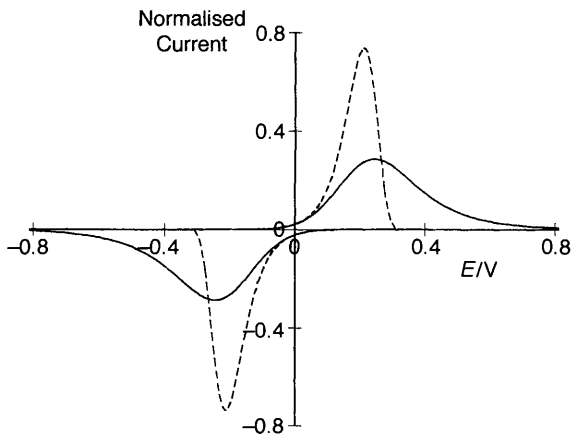

Fig. 4 A comparison of the waveshapes predicted by Marcus theory (—) and Butler–Volmer theory (---) for an 'irreversible' reaction with equal k_0 values. The Marcus reorganisation energy is 0.2 eV and the Butler–Volmer 'α' is 0.5.

predicts electrochemical rate constants by summing over all the individual rate constants for each Fermi level in the electrode as given below. The separate rate constants are the standard Marcus long-range electron-transfer rate constants specific to two energy levels: the actual rate of electron transfer from or to a specific level is influenced by the probability of occupancy of that level as predicted by the Fermi–Dirac distribution, eqn. (1).[9]

$$k_{red} = \sum_i \frac{1}{(e^{(E-E_i)F/RT}+1)} \frac{4\pi^2}{h} \times V_R^2 \frac{1}{\sqrt{4\pi\lambda RT}} e^{-[[F(E_i-E^0)+\lambda]^2/4\lambda RT]} \quad (1)$$

In this equation, k_{red} is the rate constant for reduction, E_i is the energy of a specific Fermi level, E is the applied potential, E^0 is the reduction potential of the adsorbed species, λ is the reorganisation energy and V_R^2 is a constant relating to the degree of electronic coupling. The behaviour of systems having poor electronic coupling and low reorganisation energy (*e.g.* metalloproteins) is better accounted for compared to the Butler–Volmer model, particularly under conditions of fast scan rates where the peaks occur at higher overpotential and lie more in the plateau region.

3.2 Small molecule model systems

Cyclic voltammetry and other methods such as chronoamperometry are being used to test these theoretical models using surface-confined redox systems possessing a high level of chemical definition. A general theme has been to derivatise a metal surface with a layer of bifunctional molecules as illustrated by Fig. 5. Here, a functional group such as a redox-active entity is linked to the surface *via* an alkyl spacer (CH_2) terminated by a sulfhydryl.

Several groups have studied the electrochemical kinetics of self-assembled monolayer (SAM) structures consisting of ferrocenes linked to gold through alkane thiols of varying chain length. Typically, the electrode is a gold mirror surface prepared by sputtering on silica wafers. Notably, Chidsey[9] was able to predict the variation of electron-transfer rate with free-energy and temperature, and his conclusions have been supported and extended in studies by Murray and co-workers,[15] and by Weber and Creager.[14] Another system investigated in detail features $Os^{III,II}$ complexes adsorbed on platinum.[10] Monolayer coverage of $[Os(bipy)_2Cl(X)]$ (bipy is 2,2′-bipyridyl; X is 4,4′-bipyridyl or analogues with two or three CH_2 groups spacing the pyridyl rings) is achieved at platinum microelectrodes utilising the

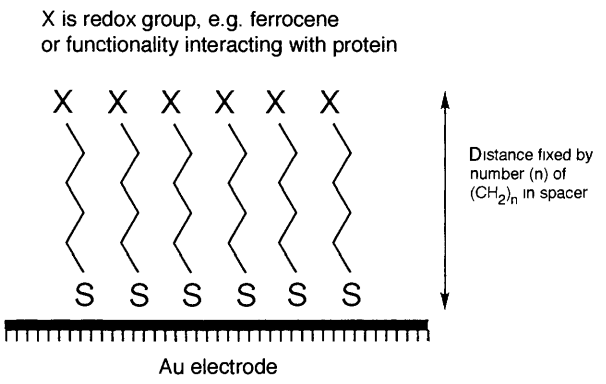

Fig. 5 Cartoon showing the structure of electrode surfaces modified with a monolayer of functionalised alkanethiolate. The group X may be redox active or a functionality such as carboxylate that is capable of interacting with the surface of a protein.

pendant pyridyl-*N* atoms from ligands X as anchors. The relatively ideal response allows detailed investigation of the effects of electrolyte, solvent, temperature and electron-transfer distance. At a sufficiently large overpotential, electrochemical rates were observed to become independent of driving force, again indicating the validity of Marcus theory. This work raises several important points relevant to observations we have made with proteins, and indicates the usefulness of such systems as models for protein film voltammetry. First, the response is asymmetric with respect to overpotential and can be modelled as a tunnelling process between electronic manifolds on either side of the interface. Secondly, a finite peak separation remains at lowest scan rates. Thirdly, the rate constant is approximately, but not completely, independent of ionic strength, raising the possibility that ion transport/binding effects are influential.

3.3 Proteins at electrodes: configurations

The concept of structurally defined monolayers has been extended to study electron transfer in protein films. Cytochrome c adsorbs strongly at SAMs prepared by treating gold mirror electrodes with ω-mercaptocarboxylic acids of the type $HS(CH_2)_nCOOH$, providing what is so far the best achievement of a protein–electrode interface having a definable structure.[11,12,16] The principle is that the carboxylates project out into the solution where they interact with the protein, presumably by salt bridging to lysines ($-NH_3^+$) located around the exposed haem edge. Bowden and co-workers have studied interfacial electron transfer in cytochrome c SAMs using cyclic voltammetry and impedance.[11,12] Protein coverages were measured independently by X-ray photoelectron spectroscopy.[11] Electroactive monolayers were obtained for films composed with SAMs having n = 15, although the rate constants were small due to poor electronic coupling. As expected, shorter chain lengths gave higher rate constants, but a smaller fraction of the adsorbed cytochrome c molecules were electroactive, suggesting incorrect orientation. Niki and co-workers have used a potential-modulated optical method (AC modulated UV–VIS electroreflectance) to calculate apparent electron-transfer rate constants for different chain lengths.[16] Although results for small chain length were lower than predicted, those for larger n agreed with distance-dependence expectations for a through-bond tunnelling mechanism.

Studies in our laboratory have focused on the use of pyrolytic graphite edge (PGE) electrodes which are prepared simply by polishing with an alumina slurry and cleaning by ultrasound. This produces a fresh, rough surface which is hydrophilic and rich in acidic oxides.[17] The roughness is probably important in enabling the irregularly shaped macromolecules to make multiple polar contacts with the electrode. Adsorption and stabilisation are optimised by low temperatures (*e.g.* 0 °C), choice of electrolyte conditions such as ionic strength, and co-adsorbates such as aminocyclitols that may create ternary salt

bridges between like-charged regions of protein molecules and electrode surface. The strategy is empirical but pragmatic. It provides a surface which has a wide potential range in aqueous solutions and is effective for a wide range of proteins, for which we are interested not so much in the mechanism of interfacial electron transfer *per se* but more in the characterisation of active sites and measurements of redox-coupled activities. We have found that a major obstacle to success is not so much electrode preparation but the failure to have samples of sufficiently high purity—denatured proteins and fragments probably tending to adsorb preferentially and attenuate the response.

3.4 The integrity of adsorbed proteins

There are several accounts of spectroscopic studies to determine the degree to which proteins retain their native structure when adsorbed at an electrode. Surface-enhanced Raman spectroscopy has been used to study cytochromes adsorbed at silver.[18,19] These experiments have revealed that the native state can be preserved even at an unmodified metal electrode. Cytochrome c_3 exhibits particular robustness, while for mitochondrial cytochrome c, structural changes do occur but depend on the electrode potential that is applied. Hinnen and Niki have used electroreflectance to examine cytochrome c at modified metal surfaces[20] while Bowden's group have studied cytochrome c adsorbed at optically transparent indium tin oxide.[21] The intense Soret absorption band provides an excellent spectroscopic handle even though the quantity of sample in a monolayer is so small. It was concluded that little alteration in the haem environment occurs upon adsorption at this hydrophilic surface.

An obvious key factor is the degree to which the reactivities observed in the adsorbed state compare with those characteristic of the protein when free in solution. These quantities can range from reduction potentials of well-characterised systems, to rate and equilibria data for coupled reactions. Small discrepancies in the reduction potential are easily tolerated given that the more robust and characteristic chemical properties are maintained. In general, a certain degree of alteration is expected because of the special nature, *e.g.* field inhomogeneity, of an interfacial environment, although we decline to accept that such a medium is non-physiological since so many biological processes occur at comparable interfaces *e.g.* membranes and large protein surfaces. As an example, cytochrome c adsorbed at a gold/alkanethiolate SAM surface exhibits a reduction potential of 215 mV compared to the value of 260 mV characteristic of the protein in solution: however the surface-adsorbed value is closer to data determined for cytochrome c bound at biological interfaces, for example 225 mV when complexed with cytochrome c oxidase.[11] For enzymes, the situation is more easily assessed since one can measure and compare specific catalytic activities.

3.5 Even ill-defined protein films produce surprisingly ideal electrochemical characteristics

Protein film voltammetry at PGE electrodes produces some excellent results despite the probability that the electrode surface and protein film are very different to the flat ordered array depicted in Fig. 1. Peak widths δ measured at low scan rates are often observed to be at or just above the theoretical minimum (hence no thermodynamic dispersion). This result is not unexpected because (unlike small molecules) the redox centres are well separated by the insulating protein matrix and their local environments are defined independently of solvent–solute interactions. However, there are deviations from ideal behaviour, such as asymmetry between oxidative and reductive scans, that may be attributable to conformational changes in the adsorbed state, or to asymmetry in the electron-transfer characteristics as has been observed for osmium monolayers at platinum.[10] However, this does not greatly detract from the basic results of our experiments; indeed we have been able to achieve cyclic voltammetry of adsorbed proteins at scan rates in the region of 1000 V s^{-1}. Fig. 6 shows the voltammetry of *Pseudomonas aeruginosa* Azurin, a 'blue' copper protein, measured at 500 V s^{-1}. The timescale is now fast enough to render any coupled reactions on the millisecond timescale as rate limiting and thus gating. Such reactions, if they occurred, would remain unnoticed and unaddressed by static electrochemical methods or indeed by conventional voltammetry which relies on sluggish protein diffusion. In summary, it is becoming clear that electron exchange between an electrode and an adsorbed protein may be extremely facile, thus enabling investigations to focus upon the characteristics of the protein itself.

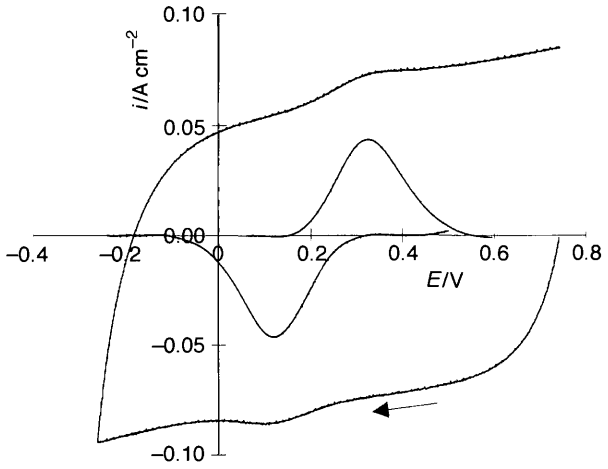

Fig. 6 Rapid cyclic voltammetry of *Pseudomonas aeruginosa* Azurin, a 'blue copper' protein, at 500 V s^{-1}, pH 8.0, 0 °C. Baseline subtracted peaks (not to scale) are shown in the centre of the voltammogram.

4 The film voltammogram as a 'spectrum'

An obvious and straightforward application of protein film voltammetry is to use the voltammetric signals (*i.e.* a pair of oxidation–reduction peaks) as electrochemical markers for identifying and quantifying the status of centres present within the protein. In effect, this amounts to an interactive 'spectrum', but in stating this we note that voltammograms provide no structural information. Assignment of signals thus depends on the use of true spectroscopic methods such as EPR to examine species generated in solution at corresponding potentials.

4.1 A sensitive method for observing Fe/S clusters and characterising their redox chemistry

Iron–sulfur (Fe/S) clusters are well established as electron-transfer centres, but much less is known about their atom-transfer properties, *i.e.* their abilities, in different proteins, to undergo changes in composition and ligation. Iron–sulfur clusters generally lack characteristic spectral features useful for real-time monitoring, and their reactivities depend critically upon oxidation level, thereby creating problems that can render conventional investigative strategies ineffective. Protein-film voltammetry provides a way to control the chemistry through the applied potential and observe the cluster transformations that are induced.[22–24] The spectrum analogy is well demonstrated for proteins that contain several such centres. Fig. 7 shows a voltammogram obtained at 20 mV s^{-1} for a small negatively charged protein (a ferredoxin from *Sulpholobus acidocaldarius*) containing a [3Fe-4S] cluster and a [4Fe-4S] cluster.[25] The film, displaying activity corresponding to monolayer coverage, was formed at a PGE electrode, at 0 °C and in the presence of polymyxin. Signals from the two centres are simultaneously visible and their distinctive redox characteristics are apparent from simple inspection. Signals A′ and B′ have been respectively assigned to the redox couples $[3Fe\text{-}4S]^{1+/0}$ and $[4Fe\text{-}4S]^{2+/1+}$ on the basis of correspondence with species generated electrochemically as free solution species and

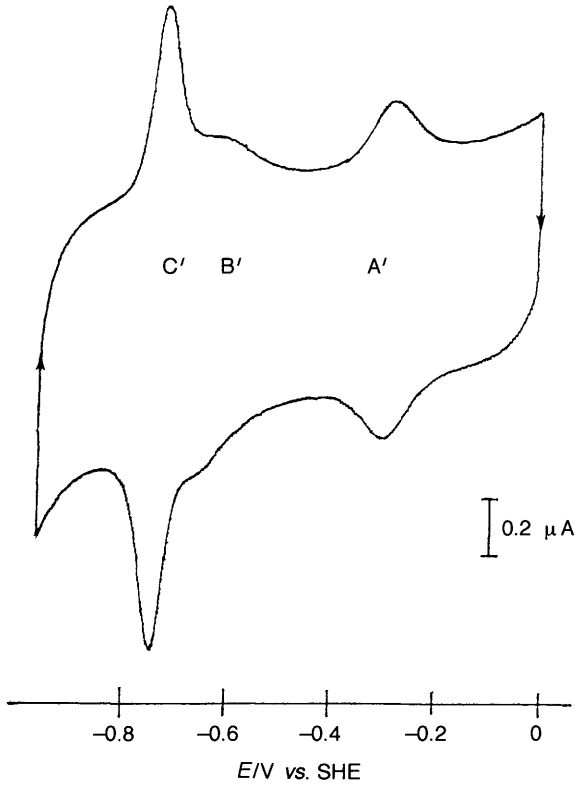

Fig. 7 The voltammogram as a spectrum: Film voltammogram of the 7Fe ([3Fe-4S] + [4Fe-4S]) ferredoxin from *Sulfolobus acidocaldarius*. Signals A′, B′ and C′ correspond to the couples $[3Fe\text{-}4S]^{1+/0}$, $[4Fe\text{-}4S]^{2+/1+}$ and $[3Fe\text{-}4S]^{0/2-}$.

characterised by EPR and MCD spectroscopy.[25] The voltammogram reveals novel redox activity: signal C′ corresponds to the couple $[3Fe\text{-}4S]^{0/2-}$ which, as a two-electron reaction involving multiple proton transfer, has no precedent in Fe/S chemistry. The C′ signal appears for other proteins containing [3Fe-4S] clusters: using the ferredoxin from *Sulpholobus acidocaldarius*, the hyper-reduced form $[3Fe\text{-}4S]^{2-}$ has been generated electrochemically in solution and partially characterised by adsorption, EPR and MCD spectroscopies.[26]

Closer inspection shows how well the voltammetry conforms to the expectations outlined earlier. Signal A′ has half-height widths of 90–100 mV at modest scan rates, thus showing that there is little (thermodynamic) dispersion due to differing orientations and environments. Signal C′ is much sharper, with the reductive peak having a half-height width of 50 mV and charge integral twice that of A′. Indeed, as examined by voltammetry, appearance of the two signals, A′ (one-electron) and C′ (intense, narrow two-electron signal) constitutes the characteristic signature of a [3Fe/4S] cluster.[26] Signal B′ appears as a shoulder on the side of signal C′ but is nevertheless clearly defined. The surface coverage based on integration of signal A′ and assuming a geometric electrode area equates to an area of *ca.* 600–700 Å^2 per protein molecule: perhaps fortuitously, this value is approximately as expected for a flat monolayer. The peak separations associated with signals A′ and B′ remain small even at scan rates in excess of 10 V s^{-1}, whereas signal C′ undergoes complex changes. These observations relate to the rate and extent of coupling of electron transfer. The redox couple $[4Fe\text{-}4S]^{2+/1+}$ is a 'pure' electron transfer reaction, while $[3Fe\text{-}4S]^{1+/0}$ involves rapid coupled proton transfer. By contrast the $[3Fe\text{-}4S]^{0/2-}$ couple is complicated by coupling to slow, pH-dependent chemical reactions.

5 Coupled reactions—non-catalytic

The capability for achieving precise temporal control of electron transfer enables complex redox-coupled chemical reactions to be studied. In effect, the experiment involves causing an electron (or hole) to cross the electrode–protein interface and then 'calling it back' after a brief period of time. Transient species can be detected and rate constants determined, the upper limits of which will certainly increase as technical developments improve the experimental timescale. The kinetic parameters fit naturally within the overall thermodynamic picture that voltammetry provides. For iron–sulfur clusters, studies have been made of the reversible binding of metal ions, H^+, and ligands, each of which display affinities and rates that depend on cluster oxidation level.

5.1 Controlling and visualising cluster transformations

The value of the voltammetric 'spectrum' is increased for proteins containing a labile centre (an analogy being that a moving object is more visible than a static one). Introduction of Zn^{2+} ions (10 μM) to the electrolyte contacting a film of the 7Fe ferredoxin from *Desulphovibrio africanus* results (Fig. 8) in rapid attenuation of signals A′ and C′ and appearance of a new signal *, as the [3Fe-4S] cluster converts to a cubane formulated as [Zn3Fe-4S] (analogous to [4Fe-4S]). Other metals give [M3Fe-4S] products having different reduction potentials.

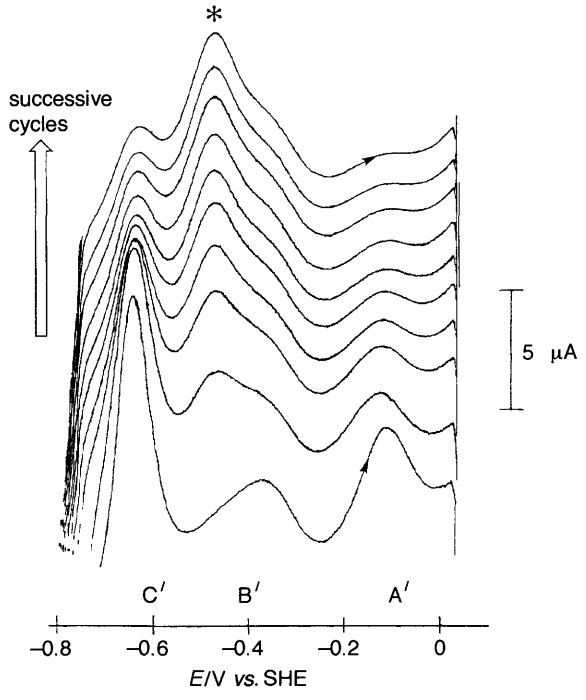

Fig. 8 Detecting interactions between redox centres and exogenous agents: Voltammograms (direction of increasing potential) obtained for a film of 7Fe ferredoxin III (*Desulfovibrio africanus*) showing the rapid reaction of $[3Fe\text{-}4S]^0$ clusters with Zn^{2+}. Signals A′ and C′ disappear, and are replaced by a signal (*) assigned to $[Zn3Fe\text{-}4S]^{2+/1+}$ partly overlaying the signal (B′) due to the inert [4Fe-4S] cluster.

The affinity of the [3Fe-4S] cluster for metal ions depends on its oxidation level. Transfer to a cell containing a complexing agent such as EGTA (or cyanide for M = Cu) and cycling to high potentials causes transformation back to $[3Fe\text{-}4S]^{1+}$. Such transformations are relevant to cluster assembly in proteins and to the emerging role of these centres in cellular sensory functions.[26]

The system is suitably described in terms of interconnected square schemes, shown in Scheme 1, in which solid arrows indicate the experimentally observed pathways. Since the entire protein sample responds immediately to the electrode potential, specific binding equilibria are addressed by holding the potential at selected values. In this way, the binding of M^{2+} ions (M = Fe, Zn and Cd) to $[3Fe\text{-}4S]^0$ producing $[M3Fe\text{-}4S]^{2+}$ could be studied quantitatively, minimising the effects of

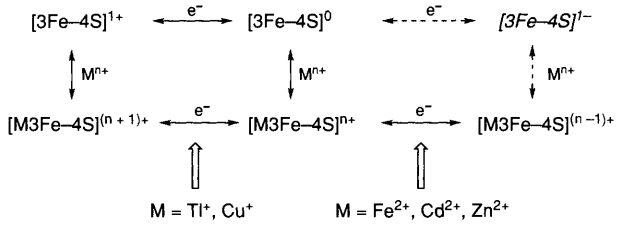

Scheme 1 Electrochemical relationships between [3Fe-4S] and [M3Fe-4S] clusters, represented by connected square schemes coupling electron transfer to metal binding

competing redox reactions. By measuring the magnitude of signals due to the cubane product [M3Fe-4S] as a function of metal ion concentration, dissociation constants K_d (= {[3Fe-4S]^0}{M^{2+}}/{[M3Fe-4S]$^{2+}$}) were determined and the affinity order Cd > Zn > Fe was deduced.[22] The ferredoxin from *D. africanus* is unusual in that the [3Fe-4S] cluster lacks a cysteine residue to coordinate the incoming metal ion, as is normally the case for a [4Fe-4S] cluster.[22] Instead, an aspartate or perhaps a water molecule completes the coordination in [M3Fe-4S], resulting in a weaker affinity for M. The controlling factor is the poor metal coordinating capability of the oxidised [3Fe-4S]$^{1+}$ cluster: application of an oxidising potential causes ejection of M, in a reaction that mimics the degradation process known to occur for 3Fe/4Fe proteins such as aconitase. Feinberg and co-workers studied this reaction in aconitase itself.[27] Although not configuring the sample as an adsorbed film, they could detect cluster interconversions occurring in solution by monitoring changes in the square-wave voltammogram.

By contrast with the relatively slow reactions observed with divalent transition metals, Tl^+ binds and dissociates much more rapidly, *i.e.* within the timescale of voltammetry performed up to a scan rate of 1 V s^{-1}.[23] During the passage of a voltammetric cycle, this system equilibrates among all the species shown in the left-hand square of Scheme 1 so that just a single signal is observed over a wide range of Tl^+ concentration. The equilibrium constants for the reactions were determined from the variation in reduction potential with Tl^+ concentration. The results showed that Tl^+ binds tightly to [3Fe-4S]^0 (K_d = 1 μM) and weakly to [3Fe-4S]$^{1+}$ (K_d = 0.1 M).

5.2 Rate-limiting proton-transfer reactions

Long-range electron-transport systems involving coupled proton transfer may be limited not by electron transfer but by the rate at which a proton can hop between bases within the protein interior. An example is the redox cycling of bound quinone in photosynthetic reaction centres in which rate-determining proton transfer to the cofactor is mediated by bases such as the side-chain carboxylates of aspartate and glutamate.[28] These are obviously gated electron-transfer reactions, the details of which can be studied by voltammetry.

The [3Fe-4S]^0 (*i.e.* one-electron reduced) cluster in various proteins binds a single proton, to produce a spectroscopically distinct form H^+-[3Fe-4S]^0.[25] The reaction is depicted in Scheme 2. For the structurally characterised 7Fe ferredoxin

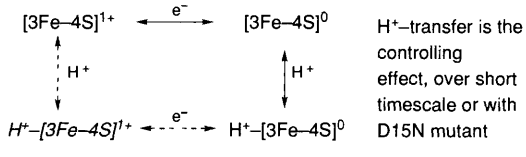

Scheme 2 Square scheme representing redox-coupled protonation in the [3Fe-4S]$^{1+/0}$ system. Slow transfer of H^+ from the [3Fe-4S]^0 cluster gates the oxidation to [3Fe-4S]$^+$.

from *Azotobacter vinelandii*, the pK for this process is 7.8, necessitating protonation even at neutral pH.[29] The [3Fe-4S] cluster is buried 8 Å below the protein surface but an aspartate carboxylate is located close to the surface in a position where it could act to mediate protons. There is no access of H_2O to the cluster, thus eliminating the possibility of H^+-mediation by water. Voltammetry reveals interesting differences between the native protein and a mutant form (D15N) in which the aspartate is replaced by asparagine. The comparison is shown in Fig. 9. The native protein shows a reversible oxidation and reduction (*i.e.* conversion between the oxidised and the reduced-protonated cluster is facile) whereas the lack of a clear oxidation wave in the D15N voltammogram reveals trapping of the reduced-protonated species by the rate-limiting excape of the proton from the cluster.[29] The fourth species, the oxidised protonated cluster, H^+-[3Fe-4S]$^{1+}$ is included in Scheme 2 in order to complete the cycle; however, rapid sweeps to high potentials have revealed no evidence for its participation. The course of the electrochemically driven cycle thus involves reduction of the cluster followed by a reversible protonation and return along the same route.

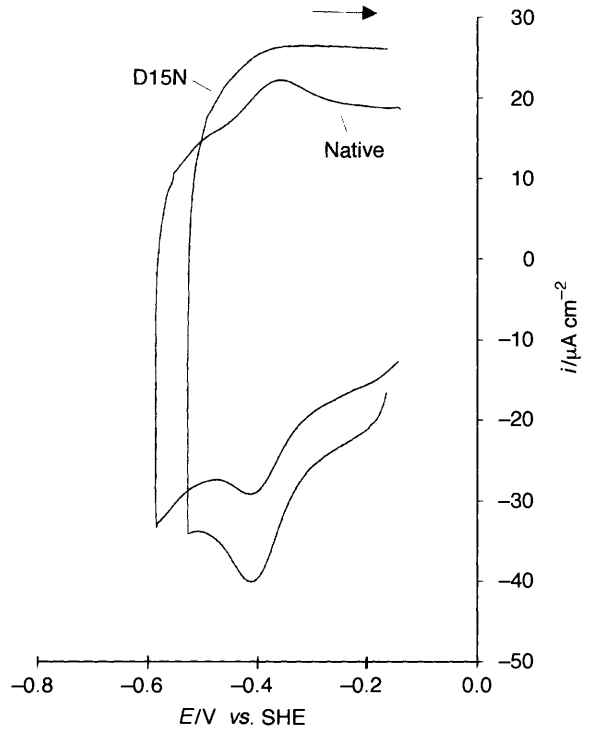

Fig. 9 Proton-gated electron transfer: Voltammograms recorded (1 V s^{-1}, 0 °C) for *Azotobacter vinelandii* 7Fe Ferredoxin I native and D15N mutant forms, revealing retardation of oxidation of [3Fe-4S]^0 upon replacement of aspartate by asparagine. D15N (pK 6.9) pH 5.5; Native (pK 7.8) pH 6.5 thus experiments performed at similar protonic driving force.

Shown in Fig. 10 is a plot of the peak positions of the oxidative and reductive waves for the D15N mutant as a function of scan rate at two pH values. At pH 8.5 (the pK for D15N is 6.9), simple electron-transfer characteristics are observed [see Fig. 2(*a*)] which can be analysed by Marcus theory.[14,15] In contrast, at pH 6.5 the behaviour is complex: at low scan rates, the voltammetry appears reversible because protonation and deprotonation of the cluster occur within the timescale of the potential perturbation. The increased reduction potential reflects the thermodynamics of the diagonal transition (the redox Bohr effect). As the scan rate is increased (all scans start at the high-potential limit, and only the initial scan is considered) the oxidation peak becomes attenuated, less defined and then vanished [as evident from Fig. 9 and depicted in Fig. 2(*b*)] because the cluster becomes trapped in the protonated form. (The second cycle reveals, as expected, that the reduction wave is also attenuated.) Finally, at high scan rate, the voltammetry reverts to that expected for electron transfer alone: the peak positions now overlay the curves observed at pH 8.5 because the scan is reversed before the reduced cluster is able to

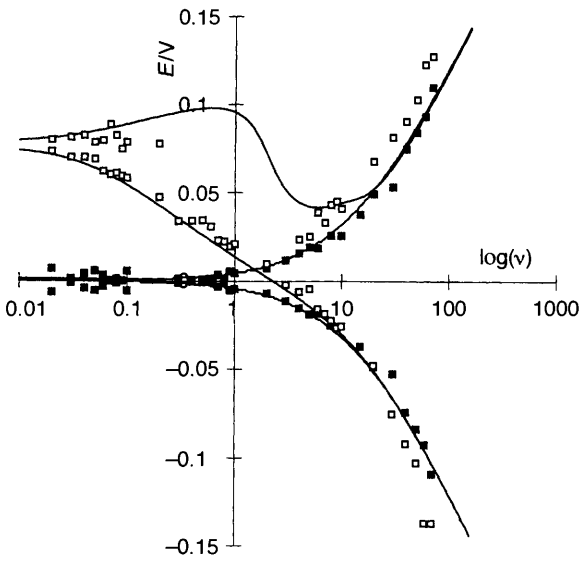

Fig. 10 Proton-gated electron transfer: Peak separations as function of scan rate for voltammetry of the $[3Fe\text{-}4S]^{1+/0}$ cluster in the D15N mutant of *Azotobacter vinelandii* Ferredoxin I. ■—data points at pH 8.5 (no protonation of $[3Fe\text{-}4S]^{0}$). □—data points at pH 6.5. The lines indicate the predictions of the square-scheme model (Scheme 2). The potential scale is with respect to the potential observed in the absence of proton transfer.

protonate. The data are modelled using rate constants for protonation and deprotonation in accordance with the pK. In this case, the rate constant for deprotonation of the cluster ($< 5\ s^{-1}$) is much slower than observed for the native protein.

Other coupled reactions of iron–sulfur clusters have been detected, and a detailed study has been carried out on the rapid and reversible binding of an exogenous thiolate ligand (RS^-) to the 2^+ and 1^+ oxidation levels of the transformed [Fe3Fe-4S] cluster in *D. africanus* ferredoxin III.[30] In this case it was possible to observe all four states of the square scheme, and to determine rates and equilibrium constants. Notably, binding of RS^- to the reduced cluster is too weak to permit its measurement by EPR, the obvious method for detecting such interactions.

6 Coupled reactions—catalysis

Studying enzymes by protein film voltammetry holds several attractions, a main feature being that kinetic measurements can be varied from steady-state to transient mode, and carried out on a minuscule population of enzyme molecules which can be interrogated at the same time to address the status of active sites. A high degree of control is exercised over the electrochemical potential and hence the driving force, although (as eluded to earlier) care is needed in order to judge that potential-independent 'limiting currents' are not the result of reaching the Marcus plateau region. Furthermore, hydrodynamic control, imposed by the rotation of the electrode, allows the substrate to be supplied to the enzyme at a given rate and enforces removal of products. The detailed catalytic waveform (shape, *i.e.* gradient, halfwave potential), its variation with conditions, and how it relates to the signals obtained in the absence of turnover, together lead to a picture that integrates both thermodynamics (reduction potentials, substrate binding) and kinetics (both of electron transfer and associated chemical events). The following examples illustrate the kind of information that can be derived.

6.1 Detection of co-operative electron transfer activity at a high-potential catalytic site

Cytochrome-c peroxidase (CCP) is a relatively small enzyme (M_W 34 000) which contains a single Fe porphyrin and catalyses the reductive breakdown of H_2O_2 by reduced cytochrome c. The catalytic cycle (see Scheme 3) involves a highly oxidising intermediate known as 'Compound I' formally at the oxidation level of Fe^V, but which actually contains Fe^{IV} and a radical cation located on a nearby tryptophan (W191). Amino acid radicals and Fe^{IV} species are each now known to be very important in oxygenative catalysis; however, the high reduction potentials and reactivities of these species have hindered quantitative studies of their redox chemistry.

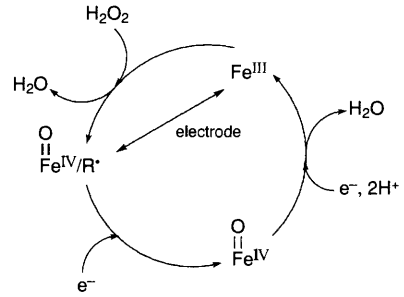

Scheme 3 The peroxidase catalytic cycle, and replacement of the chemical electron donor (cytochrome c) by an electrode

At low ionic strength and low temperature, CCP can be adsorbed on a PGE electrode.[31] In the absence of H_2O_2, a reversible signal is observed at 720 mV (pH 6.1) which transforms into a catalytic wave when H_2O_2 is added. Typical results are shown in Fig. 11. The peak signals correspond to reduction and oxidation of the catalytic machinery and provide a new means of studying the high-potential states. The half-height widths of the peaks in both directions are below the theoretical value for a one-electron redox reaction (*i.e.* $n > 1$) thus identifying them with a co-operative two-electron redox couple. The implication is that the redox activities of the haem $Fe^{IV/III}$ and Tryptophan-191 are tightly coupled. The catalytic wave produced when H_2O_2 is added arises [as described in Fig. 2(*c*)] because the H_2O_2 reaction feeds electrons back into the system. Studies carried out by varying electrode rotation rate, pH and substrate concentration show that this is a very active enzyme, equivalent or even superior to the system studied in solution with cytochrome c as electron donor.

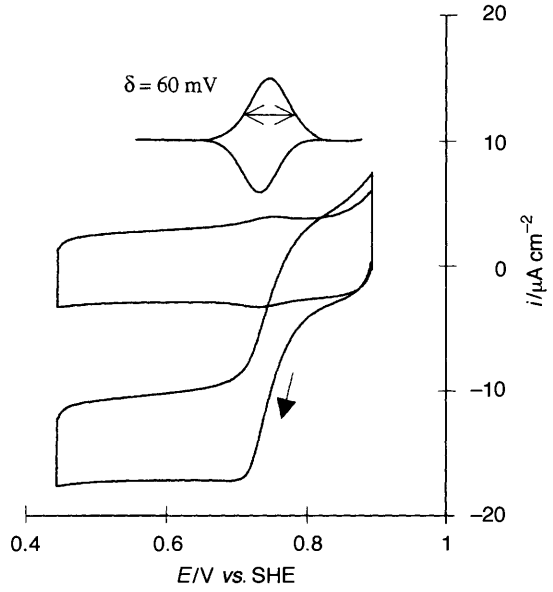

Fig. 11 Peroxidase electrocatalysis: Cyclic voltammetry of yeast cytochrome c peroxidase obtained at a rotating disc electrode, pH 6.1, (20 mV s^{-1}, 0 °C) showing how the reversible peaks transform to a catalytic wave in the presence of H_2O_2 (20 μM). Upper trace (not to scale) shows baseline-subtracted signal in absence of H_2O_2.

6.2 Delineation of electron flow patterns in multicentred enzymes

For multi-centred enzymes, the ability to control and fine-tune the electrode potential allows different redox centres to be addressed selectively, and their roles in catalysis examined. Fumarate reductase (FRD) is a multicentred enzyme catalysing the reduction of fumarate to succinate in bacterial respiratory chains.[7] It is associated with the cytoplasmic membrane and consists of four subunits, of which two form the membrane anchor and quinone binding sites. The other two subunits are membrane-extrinsic and contain three Fe-S clusters ([3Fe-4S]$^{1+/0}$, [4Fe-4S]$^{2+/1+}$ and [2Fe-2S]$^{2+/1+}$) and a covalently bound flavin (FAD). Reduction potentials of the [3Fe-4S] and [2Fe-2S] clusters (reported values at pH 7 range between −20 and −79 mV) and the flavin (−55 mV) are suited to mediate electrons between menaquinol (−73 mV) and fumarate/succinate (+30 mV) but the low potential of the [4Fe-4S] cluster (−320 mV) poses a question as to its role. The membrane-extrinsic domain can be isolated and the resulting soluble enzyme catalyses fumarate reduction by artificial electron donors. As depicted in Fig. 12, the soluble protein adsorbs at a PGE electrode, whereupon its properties are revealed in more detail.

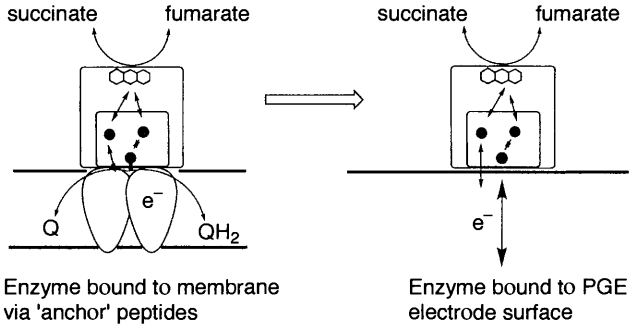

Fig. 12 Cartoon depicting fumarate reductase or succinate dehydrogenase. The two catalytic subunits containing three Fe-S clusters (small subunit) and FAD (large subunit) can be separated from the membrane-bound anchor peptides and adsorbed at an electrode.

Cyclic voltammograms measured in the absence of substrate reveal signals that can be assigned to reduction and re-oxidation of the three Fe-S clusters and the FAD.[7] Those attributable to [2Fe-2S]$^{2+/1+}$, [3Fe-4S]$^{1+/0}$ and the FAD are enveloped together in a prominent reversible signal in the region of −50 mV, the prominence being due to the n = 2 character of the FAD. A weaker signal appears at *ca.* −320 mV, corresponding to the potential expected for [4Fe-4S]$^{2+/1+}$. When a small concentration of fumarate is added, the envelope of signals at high potential transforms to a catalytic wave. At higher fumarate concentrations, this catalytic wave becomes very large and (particularly at higher pH) a second smaller catalytic wave becomes visible close to the potential of the [4Fe-4S] cluster.[7] The resulting waveform is shown in Fig. 13. From the potentials, relative intensities and shapes of the two catalytic waves under different conditions, it could be deduced that intramolecular electron transfer proceeds by two pathways (*i.e.* electrode → 2Fe/3Fe → FAD and electrode → 4Fe → FAD). The picture is enhanced by transforming the steady-state voltammogram to the derivative form where the two pathways appear as peaks. The simple catalytic wave observed at low substrate concentrations occurs because both electrons for fumarate reduction are supplied at an adequate rate by the high potential clusters. However, at high substrate concentration, the demand for electrons is greatly increased so that the [4Fe-4S] cluster is recruited, thereby resulting in a boost of turnover. Likewise, as the pH is increased, the reduction potential of the FAD decreases relative to that of the high-potential clusters making them poorer electron donors, so that activity becomes more dependent on participation of the [4Fe-4S] cluster. The

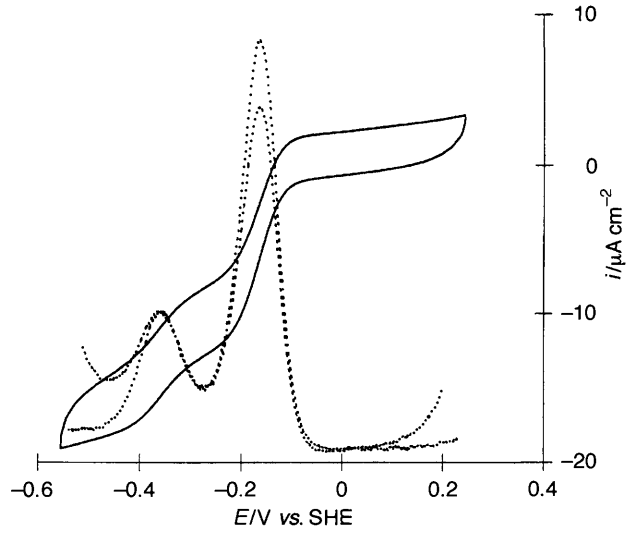

Fig. 13 Detection of electron-transfer pathways in multi-centred enzymes: (—) rotating disc cyclic voltammogram showing the reduction of fumarate (0.8 mM) by fumarate reductase, pH 9.5, 20 °C, 10 mV s^{-1}. (---) the first derivative of the voltammogram generating a 'pathways' spectrum.

results illustrate how protein-film voltammetry can be used to quantify the involvement of different centres in intramolecular electron transfer, a task that is not easily accomplished by other methods.

6.3 Detection of electron-transport switches and catalytic bias

Succinate dehydrogenase (SDH) is the soluble component of Complex II, a mitochondrial enzyme which catalyses the oxidation of succinate to fumarate in the Kreb's cycle. In terms of structure and redox centres, SDH is similar to the soluble domains of fumarate reductase. There are three Fe-S clusters and one covalently bound FAD. When examined as a protein film, several interesting features are observed, although no signals are apparent in the absence of substrate (implying that the enzyme adsorbs to give only a low electroactive coverage) and for reasons as yet unclear, the catalytic voltammetry is unstable. Shown in Fig. 14(a) are successive cyclic voltammograms recorded for a SDH film contacting a solution with equal concentrations of fumarate and succinate, *i.e.* measuring the bi-directional characteristics of the enzyme.[32,33] At first glance the voltammetry appears extremely complicated: in fact, however, the electrochemistry is even more amenable to interpretation than the enzymes described above because it is controlled entirely by the enzyme's kinetics, and not by substrate mass transport or interfacial electron exchange. Several subtle features are now revealed.

Both oxidation and reduction currents are observed but these decay with time producing isosbestic points that correspond to the substrate reduction potential $E_{F/S}$. The waveforms are not sensitive to electrode rotation rate or scan rate (at least up to 50 mV s^{-1}). Most noticeably, the fumarate reduction current reaches a maximum value at a certain potential, then decreases.[32,33] Analysis is carried out by computing difference voltammograms—subtracting later from earlier cycles—which effectively removes the background and yields a relative activity profile. From Fig. 14(b) it is seen that the enzyme activity drops to a lower level (but not zero) as the potential is made more negative. We have termed this the 'tunnel-diode' effect due to analogy with the electronic component which displays negative resistance over a limited region of potential bias. In the absence of this switch, the reduction current would continue to increase to a maximum value as indicated. It is immediately evident that, at pH 7, SDH is more proficient at catalysing in the direction of fumarate reduction even with this switch in operation. For the following reasons, the tunnel-diode

effect has been assigned to reduction of the FAD.[32] First, the results of experiments conducted over a range of pH can be modelled in terms of two states of the enzyme (active and less-active) which interconvert rapidly through a simple Nernst equilibrium. The characteristics of the redox couple responsible for this interconversion are very similar to those expected for the FAD. Secondly, the magnitudes and positions of the fumarate reduction peaks are sensitive to oxalacetate, a competitive inhibitor which is known to bind close to the FAD, but more tightly to the oxidised form. Thus, the redox state of the FAD acts as a regulator of electron transport, most likely through a subtle conformational change. A similar 'tunnel diode' effect has been reported for the voltammetry of gluconate dehydrogenase.[34]

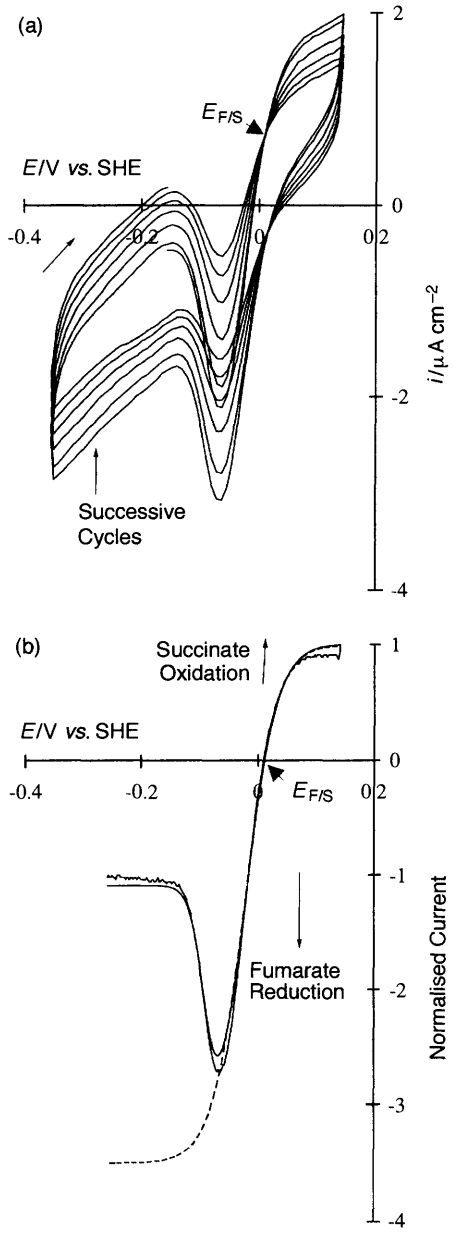

Fig. 14 Revealing a redox-state dependent activity switch: (a) Rotating disc cyclic voltammograms (10 mV s^{-1}) observed at a PGE electrode for a 1 : 1 mixture of succinate and fumarate in the presence of adsorbed beef heart mitochondrial succinate dehydrogenase. pH 7.0, 38 °C. (b) The catalytic profile or difference voltammogram for succinate dehydrogenase, derived from the voltammograms in Fig. 14(a) and the simulation (smooth curve) based on a cyclic catalytic model incorporating active and less-active states of the enzyme that interconvert according to the oxidation state of the FAD. Dashed line depicts the fumarate reduction current expected in the absence of the tunnel diode effect.

6.4 Proton transfer: the energetics of substrate–solvent isotope effects

The final experiments described in this Review concern the effects of isotopic substitutions on voltammetric waveforms. The key issue is the ability to measure, simultaneously, contributions due to kinetics and thermodynamics, and to correlate these with perturbations of the active site as well as substrate transformation. Numerous conventional kinetic studies have utilised H/D substitution, both in substrate and solvent, as a mechanistic tool. These substitutions have a marked influence on the steady-state waveforms displayed by SDH, and show that catalytic electron transport in both directions is controlled by proton transfer.[35] First, dealing with the 'substrate' isotope effect, substitution of succinate and fumarate by their perdeuterated forms produces a large (*ca.* four-fold) decrease in oxidation rate but no effect on reduction. Second, addressing the 'solvent' isotope effect, substitution of H_2O by D_2O attenuates the reaction rate in both directions. Isotope effects can arise from changes in both thermodynamics or kinetics, and solvent substitutions can influence intrinsic enzyme properties, particularly reduction potentials and p*K* values, in addition to primary (kinetic) substrate effects. By examining the waveforms obtained over a range of pL (pH, pD) for 1 : 1 fumarate–succinate mixtures either in 100% H or 100% D systems, the energetics of the overall system have been compared. The consensus voltammograms (simulations) are displayed in Fig. 15. Points to note are that in the 100% D system, the potential of the peak (reflecting the reduction potential of the FAD) increases by 20 mV whereas that for fumarate–succinate (the isosbestic potential) is increased by 43 mV. The net result is that SDH becomes even more biased toward being a 'fumarate reductase', although this is a relative effect since electron transport in the fumarate reduction direction is also retarded by H/D substitution.

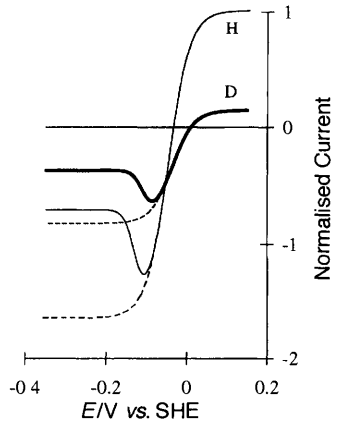

Fig. 15 Isotope effects on catalytic electron transport: consensus effects on the catalytic voltammetry of succinate dehydrogenase, of deuterating both the solvent and the succinate–fumarate substrates: S_H/F_H, H_2O (faint line), S_D/F_D, D_2O (bold line). Dashed lines denote the voltammograms expected if activity was not curtailed by the tunnel diode effect. Conditions: pH = pD = 7.4, 1 : 1 fumarate/succinate, 38 °C.

7 Summary

This Review has outlined some ideas and described a number of experiments illustrating the results that can be obtained with protein film voltammetry. What of the future? We hope to have convinced readers of the merits for fundamental studies. As has been mentioned by numerous authors, applications could include biosensors, although this would necessitate the development of systems that are stable. With stability and reproducibility established, enzymes linked to medical problems might be screened directly to obtain a 'direct read out' of the malfunction: obviously, in this way an enzyme is effectively integrated into

the electronic circuitry of an analytical instrument. Efforts are needed to understand and improve the structure of the protein–electrode interface. It will be of great interest to obtain direct structural insight into how protein molecules are actually arranged together at electrode surfaces, not only the better-behaved systems that we have focused on above, but also those that give poor or unstable activity. The successful application of scanning probe microscopy to this task will provide a major step forward in understanding and improving the methodology. Certainly, greater use will be made of spectroscopic methods such as electroreflectance whereby a potential modulation is applied to activate specific centres and measure their spectra and kinetics. With regard to subjects for study, there need be no limit, except to restate our earlier point, that it is with the more complex and intractable problems that voltammetry can come into its own.

8 Acknowledgements

Research in the authors' laboratory is supported by the Wellcome Trust and by the EPSRC. We thank Julea Butt, Jill Duff, Sarah Fawcett, Guy Jameson, Lisa Martin, Madhu Mondal and Artur Sucheta for their efforts in carrying out much of the research described. We also thank Brian Ackrell, Jacques Breton, Barbara Burgess, Andrew Thomson and Joel Weiner for their help and collaboration.

9 References

1 M. J. Eddowes and H. A. O. Hill, *J. Am. Chem. Soc.*, 1979, **101**, 4461.
2 P. Yeh and T. Kuwana, *Chem. Lett.*, 1987, 1145.
3 E. Laviron, in *Electroanalytical Chemistry*, ed. A. J. Bard, Marcel Dekker, New York, 1982, vol. 12, pp. 53–157.
4 B. S. Brunschwig and N. Sutin, *J. Am. Chem. Soc.*, 1989, **111**, 7454.
5 A. M. Bond and K. B. Oldham, *J. Phys. Chem.*, 1983, **87**, 2492.
6 F. A. Armstrong, *J. Biol. Inorg. Chem.*, 1997, **2**, 139.
7 A. Sucheta, R. Cammack, J. Weiner and F. A. Armstrong, *Biochemistry*, 1993, **32**, 5455.
8 J. H. Reeves, S. Song and E. F. Bowden, *Anal. Chem.*, 1993, **65**, 683.
9 C. E. D. Chidsey, *Science*, 1991, **251**, 919.
10 R. J. Forster and L. R. Faulkner, *J. Am. Chem. Soc.*, 1994, **116**, 5444; R. J. Forster and L. R. Faulkner, *J. Am. Chem. Soc.*, 1994, **116**, 5453; R. J. Forster and J. P. O'Kelly, *J. Phys. Chem.*, 1996, **100**, 3695.
11 S. Song, R. A. Clark, E. F. Bowden and M. J. Tarlov, *J. Phys. Chem.*, 1993, **97**, 6564.
12 T. M. Nahir and E. F. Bowden, *J. Electroanal. Chem.*, 1996, **410**, 9.
13 R. A. Marcus and N. Sutin, *Biochim. Biophys. Acta*, 1985, **811**, 265.
14 K. Weber and S. E. Creager, *Anal. Chem.*, 1994, **66**, 3164.
15 L. Tender, M. T. Carter and R. W. Murray, *Anal. Chem.*, 1994, **66**, 3173.
16 Z. Q. Feng, S. Imabayashi, T. Kakiuchi and K. Niki, *J. Electroanal. Chem.*, 1995, **394**, 149.
17 F. A. Armstrong, *Struct. Bond.*, 1990, **72**, 137.
18 P. Hildebrandt and M. Stockburger, *Biochemistry*, 1989, **28**, 6710.
19 K. Niki, Y. Kawasaki, Y. Kimura, Y. Higuchi and N. Yasuoka, *Langmuir*, 1987, **3**, 982.
20 C. Hinnen and K. Niki, *J. Electroanal. Chem.*, 1989, **264**, 157.
21 M. Collinson and E. F. Bowden, *Anal. Chem.*, 1992, **64**, 1470.
22 J. N. Butt, F. A. Armstrong, J. Breton, S. J. George, A. J. Thomson and E. C. Hatchikian, *J. Am. Chem. Soc.*, 1991, **113**, 6663.
23 J. N. Butt, A. Sucheta, F. A. Armstrong, J. Breton, A. J. Thomson and E. C. Hatchikian, *J. Am. Chem. Soc.*, 1991, **113**, 8948.
24 J. N. Butt, J. Niles, F. A. Armstrong, J. Breton and A. J. Thomson, *Nature Struct. Biol.*, 1994, **1**, 427.
25 J. L. Breton, J. L. C. Duff, J. N. Butt, F. A. Armstrong, S. J. George, Y. Pétillot, E. Forest, G. Schäfer and A. J. Thomson, *Eur. J. Biochem.*, 1995, **233**, 937.
26 J. L. C. Duff, J. L. J. Breton, J. N. Butt, F. A. Armstrong and A. J. Thomson, *J. Am. Chem. Soc.*, 1996, **118**, 8593.
27 J. Tong and B. A. Feinberg, *J. Biol. Chem.*, 1994, **269**, 24920.
28 P. H. McPherson, M. Schonfeld, M. L. Paddock, M. Y. Okamura and G. Feher, *Biochemistry*, 1994, **33**, 1181.
29 J. N. Butt, A. Sucheta, L. L. Martin, B. Shen, B. K. Burgess and F. A. Armstrong, *J. Am. Chem. Soc.*, 1993, **115**, 12587.
30 J. N. Butt, A. Sucheta, F. A. Armstrong, J. Breton, A. J. Thomson and E. C. Hatchikian, *J. Am. Chem. Soc.*, 1993, **115**, 1413.
31 M. S. Mondal, H. A. Fuller and F. A. Armstrong, *J. Am. Chem. Soc.*, 1996, **118**, 263.
32 J. Hirst, A. Sucheta, B. A. C. Ackrell and F. A. Armstrong, *J. Am. Chem. Soc.*, 1996, **118**, 5031.
33 A. Sucheta, B. A. C. Ackrell, B. Cochran and F. A. Armstrong, *Nature*, 1992, **356**, 361.
34 T. Ikeda, S. Miyoaoka and K. Miki, *J. Electroanal. Chem.*, 1993, **352**, 267.
35 J. Hirst, B. A. C. Ackrell and F. A. Armstrong, *J. Am. Chem. Soc.*, 1997, **119**, in press.

Received, 15th January 1997
Accepted, 14th March 1997